Stem Cells Express, published online November 10, 2005; doi:10.1634/stemcells.2005-0403

Original Article

Accumulated Chromosomal Instability in Murine Bone Marrow Mesenchymal Stem Cells Leads to Malignant Transformation

Masako Miura[1], Yasuo Miura[1], Hesed M. Padilla-Nash[2], Alfredo A. Molinolo[3], Baojin Fu[4], Vyomesh Patel[3], Byoung-Moo Seo[1], Wataru Sonoyama[1], Jenny J Zheng[5], Carl C. Baker[4], Wanjun Chen[6], Thomas Ried[2], Songtao Shi[1]

[1]Dental Biology Unit, [3]Oral and Pharyngeal Cancer Branch, [6]Oral infection and Immunity Branch, National Institute of Dental and Craniofacial Research, National Institutes of Health, Bethesda, Maryland 20892, USA.
[2]Genetics Branch, Center for Cancer Research, National Cancer Institute, National Institutes of Health, Bethesda, Maryland 20892, USA.
[4]Laboratory of Cellular Oncology, Center for Cancer Research, National Cancer Institute, National Institutes of Health, Bethesda, Maryland 20892, USA.
[5]Office of Clinical Pharmacology and Biopharmaceutics, Center for Drug Evaluation and Research, Food and Drug Administration, Rockville, Maryland 20850, USA.

Running title: malignant transformation of mesenchymal stem cells

Key words: bone marrow-derived mesenchymal stem cell (BMMSC), malignant transformation, chromosomal instability, fibrosarcoma

Abbreviations: BMMSC, bone marrow-derived mesenchymal stem cell.

Received August 19, 2005; accepted for publication October 31, 2005.

Abstract:

Despite recent emerging evidences suggest that cancer stem cells subsist in a variety of tumors, it is not yet fully elucidated whether postnatal stem cells are directly involved in tumorigenesis. We used murine bone marrow-derived mesenchymal stem cells (BMMSCs) as a model to test a hypothesis that tumorigenesis may originate from spontaneous mutation of stem cells. In this study, we demonstrated that murine BMMSCs, after numerous passages, obtained unlimited population doublings and proceeded to a malignant transformation state, resulting in fibrosarcoma formation *in vivo*. Transformed BMMSCs colonized to multiple organs when delivered systemically through the tail vein. Fibrosarcoma cells formed by transformed BMMSCs contained cancer progenitors, which were capable of generating colony clusters *in vitro* and fibrosarcoma *in vivo* by the second administration. The mechanism by which BMMSCs transformed to malignant cells was associated with accumulated chromosomal abnormalities, gradual elevation in telomerase activity, and increased c-myc expression. Moreover, BMMSCs and their transformed counterpart, fibrosarcoma-forming cells, demonstrated different sensitivity to anti-cancer drugs. BMMSCs/fibrosarcoma transformation system may provide an ideal system to elucidate the mechanism of how stem cells become cancer cells and to screen anti-sarcoma drugs.

Correspondence:

Songtao Shi D.D.S., Ph.D.

Dental Biology Unit, National Institute of Dental and Craniofacial Research, National Institutes of Health

Building 30, Room 131, 30 Convent Drive MSC4320, Bethesda, Maryland 20892, USA.

Phone; 301-435-4584

Fax; 301-480-5353

E-mail; sshi@mail.nih.gov

Introduction

Recently, the possibility that tumors originate from cancer stem cells has been proposed based on the fact that only a small percentage of cancer cells form tumors and that tumor cells exhibit stem cell properties such as hierarchical self-renewal, unlimited proliferation, differentiation capabilities, and utilizing stem cell associated signaling pathways to maintain “stemness” (1). Although cancer stem cells have been reported in leukemia (2-4), breast cancer (5), and brain tumor (6, 7), the exact origin of cancer stem cells remains unclear. In this study, we tried to assess whether bone marrow-derived mesenchymal stem cells (BMMSCs) are indeed involved, at least in part, in the generation of cancer stem cells because long-living stem cells may have higher probability of accumulating mutations, resulting in tumorigenesis. To date, however, it is not clear whether postnatal stem cells can be transformed to malignant cells under the standard culture conditions without any genetic manipulation, exposure to viruses, and irradiation. Given the recent report that bone marrow-derived cells contribute to gastric cancer formation (8) and human mesenchymal stem cells may be transformed to cancer cells (9), it is important to further explore the role if any, of bone marrow-derived stem cells promoting tumor formation. It has been reported that mouse embryonic fibroblasts were able to become established lines with a constant or rising growth rate following continuous *in vitro* culturing (10), implying a possibility of spontaneous immortalization of murine BMMSCs under similar culture conditions.

In the mean time, multipotent adult progenitor cells (MAPCs) were discovered as an infrequent population of BMMSCs maintained in the adult bone marrow compartment (11). They are considered as an extremely important stem cell resource for regenerative medicine since they were reported to possess pluripotent stem cell characteristics, similar to embryonic stem cells (ES cells); they differentiate into endoderm-, mesoderm-, and ectoderm-derived cells and proliferate extensively without entering into senescence. However, it is important to further verify characteristics of the cells with extensive proliferation in adult bone marrow.

In this study, we found that continuous passages led BMMSCs to spontaneous immortalization. Following additional passages, the immortalized BMMSCs became transformed into malignant cells, capable of forming fibrosarcomas *in vivo*, at least partially, due to accumulated chromosomal abnormalities, amplified c-Myc expression, and elevated telomerase activity. This consecutive conversion of BMMSCs to malignant cells provides an excellent model to study the mechanisms associated with the tumorigenic potential of postnatal stem cells and explore therapeutic strategies for malignant tumors.

Materials and Methods

Mouse BMMSC culture. Preparation and expansion of the murine BMMSCs was done based on published method (12). Briefly, bone marrow cells from adult C57Bl/6 mice were seeded into culture dishes, incubated for 4 hours and washed twice with α-MEM (Gibco BRL; Invitrogen Corp. Grand Island, NY). The culture medium consisted of α-MEM, 20% fetal bovine serum (FBS; Equitech-Bio, Kerrville, TX), 2 mM L-glutamine (Biofluids, Rockville, MD), a combination of 100 U/ml penicillin and 100 μg/ml streptomycin (Biofluids) and 55 μM 2-mercaptoethanol (Gibco BRL). Primary cultures (passage 0; P0) were passaged to disperse the colony-forming cells and seeded on freshly prepared culture dishes (P1). Initially BMMSCs were passed at 1:2-5 dilution when they reached confluent. After BMMSCs were immortalized (around P15), cells were passed at 1:10-20. To obtain single colony-derived BMMSC clones, bone marrow cells were seeded at 1-3X10^6 cells in 15cm culture dish and cultured as described above. Colonies were isolated at 14 to 21 days post cultivation. The proliferation rate of BMMSCs was assessed by bromodeoxyuridine (BrdU) incorporation for 4 hours using a BrdU staining Kit (Zymed Laboratories Inc.). *In vitro* osteogenic, adipogenic, and chondrogenic assays were done as previously reported (13, 14).

Human mesenchymal stem cell culture. Human bone marrow aspirates from healthy adult volunteers were purchased from AllCells, LLC (Berkeley, CA). To identify putative BMMSCs, single-cell suspension of 1x10^6 of bone marrow mononuclear cells (BMNCs) was seeded into 15cm culture dishes and non-

adherent cells were removed after 4 hours of incubation at 37^{o}C. The adherent cells were cultured with α-MEM supplemented with 15% FBS, 100 μM L-ascorbic acid 2-phosphate (Wako Pure Chemical Industries Ltd, Osaka, Japan), 2 mM L-glutamine, and a combination of 100 U/ml penicillin and 100 μg/ml streptomycin. BMMSCs were plated at 1:4 dilution when the cells were approaching confluence. Isolation of dental pulp stem cells and periodontal ligament stem cells were described as previously (15) (16). They were cultured in the same medium as that used for human BMMSCs and plated at 1:4 dilution when the cells were approaching confluence.

Transplantation and injection of BMMSCs. Approximately 2-4x10^{6} of murine BMMSCs were transplanted into 6-8 week-old immunocompromised (bg-nu/nu-xid) mice using hydroxyapatite/tricalcium phosphate (HA/TCP) ceramic powder (Zimmer Inc, Warsaw, IN) and harvested at 8 week post transplantation (17). To assess tumorigenesis and migration potential, 1x10^{6} of BMMSCs were injected into bg-nu/nu-xid mice subcutaneously and intravenously through tail vein, respectively. In some experiments, tumor cells were dispersed by digesting tumors with 3 mg/ml collagenase type I (Worthington Biochem, Freehold, NJ) and 4 mg/ml dispase (Boehringer Mannheim, GmbH, Germany). Then tumor cells were injected subcutaneously into second recipient bg-nu/nu-xid mice. These procedures were performed in accordance to specifications of an approved small animal protocol (NIDCR #04-317).

Histological analysis. Transplants were harvested and demineralized with 10% EDTA before embedding. The paraffin-embedded sections were stained with

hematoxylin and eosin (H&E), Mallory trichrome, or incubated with the antibodies for vimentin (Zymed Laboratories Inc. South San Francisco, CA) and cytokeratin (DakoCytomation, Glostrup, Denmark).

Fluorescence-activated cell sorting (FACS) analysis. Cells ($1X10^6$) were incubated with 1 μg of phycoerythrin (PE)-conjugated antibodies for 45 min at 4 ^oC. PE-conjugated isotype-matched IgG was used as control. Antibodies against CD45, TER119, CD13, Sca-1, Thy-1, CD34, c-kit, CD19, CD3, and CD18 were from BD Biosciences, and SSEA-1 and Flk-1 were from Santa Cruz Biotechnology, Inc. (Santa Cruz, CA).

Spectral karyotyping (SKY) and fluorescent in situ hybridization (FISH). Metaphase chromosomes for SKY hybridization were prepared from BMMSCs at different passages. Cells in culture were incubated for 1 to 2 hours in 0.02 mg/ml Colcemid (Invitrogen, Carlsbad, CA, USA). The cells were incubated in hypotonic solution (0.075 M KCl) and fixed in methanol : acetic acid (3 : 1). SKY was then performed as described previously, using a combination of five different fluorochromes (18, 19). Images were acquired with Sky^{TM} acquisition software (Applied Spectral Imaging, Ltd, Migdal Haemek, Israel) using a spectral cube and a CCD camera (Hamamatsu, Bridgewater, NJ, USA) connected to a DMRXA microscope (Leica Imaging Systems, Cambridge, U.K.) with a custom SKY-3 optical filter (Chroma Technology). A minimum of 10 metaphases was imaged and karyotyped using SkyView ^{TM} v 1.6.2 software. To confirm the origin of the double minute chromosomes detected by SKY, dual-color FISH was performed with a chromosome painting probe for chromosome MMU15 and the *c-myc* gene.

DNA was isolated from the BAC clone for c-*myc* (D15Mit17) and labeled with biotin-16-dUTP (Roche Biomolecular) using a standard nick-translation protocol. Chromosome painting probe for MMU15 (directly labeled with Cy5) used for FISH hybridizations was prepared using the same protocols as for labeling of SKY chromosome painting probes (www.riedlab.nci.nih.gov/protocols.asp). FISH probe for c-myc was labeled by Nick translation with biotin-16-dUTP (Roche BioMolecular) and visualized using the softwareCW4000 FISH (Leica Imaging Systems). The condition for hybridization was as described in http://www.riedlab.nci.nih.gov/protocols.asp.

Western blot analysis. Cells were lysed in M-PER extraction reagent (Pierce Chemical Co., Rockford, IL). Ten micrograms of protein per each lane were separated by SDS-PAGE, transferred to a nitrocellulose membrane and probed with c-Myc (Santa Cruz Biotechnology, Inc.) and β-Actin (Sigma, St. Louis, MO). Bound antibodies were revealed with goat anti-mouse IgG conjugated to HRP (Santa Cruz Biotechnology, Inc.) and blots were developed using Super Signal chemiluminescence HRP substrate (Pierce Chemical Co.).

Quantitative telomerase activity assay. The telomerase activity was evaluated using the two-step Q-TRAP assay as reported previously with slight modification (20). Briefly, 40 µl first-step reaction mixture, which contained 2.0 µg of cell lysate diluted into 26 µl of 0.1 mg/ml BSA, 1X TRAP standard reaction buffer, 50 µM of each deoxynucleotide triphosphate, 0.1 µg of TS oligonucleotide substrate (TS primer; AATCCGTCGAGCAGAGTT), and 0.2 µg of T4 gene protein (Amersham Pharmacia Biotech, Piscataway, NJ), was incubated at 33°C for 5 hours and

95°C for 10 min. Sybr Green real-time Q-PCR assays (PE applied Biosystems, Foster City, CA) were carried out using 25 μl volume containing 1.0 μl of the product from the first step and 300 nM TS and ACX primers (ACX primer; GCGCGGCTTACCCTTACCCTTACCCTAACC). Standard curve was produced for the assay using serially diluted 293 cell extracts and all samples were run in triplicate.

Telomere length assay. Genomic DNA was purified from BMMSCs using High Pure PCR Template Preparation Kit (Roche Applied Science, Mannheim, Germany). Telomere length was assessed by Telo TAGGG Telomere Length Assay kit (Roche Applied Science) according to the manufacturer's protocol.

Anti-cancer drug treatment. BMMSCs at P1 and transformed BMMSCs at P63 seeded in 96-well plates were treated with etoposide (Alexis Biochemicals, San Diego, CA; 0-1000 μg/ml) and doxorubicin (Sigma; 0-30 μg/ml) for 48 hours at 37^{o}C. Cell viability was measured by using the Cell Counting Kit-8 from Dojindo Molecular Technologies, Inc. (Gaithersburg, MD) according to the manufacturer's protocol. The inhibition effects of drugs (% of control) were calculated as (absorbance of non-treated cells - absorbance of treated cells)/absorbance of non-treated cells. EC_{50} is the drug concentration at which the cell viability becomes 50% of non-treated cells. The experiments were repeated three times. The representative plates were scanned after the reaction.

Result

BMMSCs were spontaneously transformed into malignant cells by continuous passage *in vitro*. BMMSCs from adult C57Bl/6 mice were passaged continuously for over a year and obtained unlimited population doublings (Fig. 1A). After additional passages, BMMSCs gradually acquired increased proliferating capacity as shown by BrdU incorporation (Fig. 1B). Initially, BMMSCs at P0 formed single colony clusters (Fig. 1C) and showed multiple *in vitro* differentiation capabilities to become osteogenic (Fig. 1D), adipogenic (Fig. 1E) and chondrogenic cells (Fig. 1F) under various inductive conditions (21-24). Upon *in vivo* transplantation into immunocompromised mice (17), BMMSCs at P1 (Fig. 1G) generated bone and associated marrow components, indicating an *in vivo* osteogenic differentiation capacity (Fig. 1K). BMMSCs at early stages (P2-P5) demonstrated a slower proliferation rate and an enlarged, flattened cellular morphology, indicative of cellular senescence. However, they gradually gained rapid proliferating ability after overcoming the crisis phase with continuous regular passages (10). At P13, BMMSCs still maintained a large cell morphology (Fig. 1H) but failed to generate any mineralized tissues *in vivo* (Fig. 1L), suggesting that BMMSCs have lost their osteogenic differentiation potential after they overcome the crisis phase and acquired proliferating capacity. With further continued passages (P29), the cells became smaller (Fig. 1I) and generated tumors upon *in vivo* transplantation (Fig. 1M). Moreover, as the passage number increased to P54, the cells showed a

significantly smaller morphology (Fig. 1J) and formed tumors with a shorter latent period following transplantation compared to P29 (Fig. 1N), indicating a higher degree of malignancy.

Transformed BMMSCs generated fibrosarcomas and colonized in multiple organs *in vivo*. The tumors generated by transformed BMMSCs were composed of spindle-shaped and round atypical cells and extensively invaded the surrounding muscles and subcutaneous tissues (Fig. 2A). The blue cytoplasmic staining of tumor cells by Mallory trichrome staining suggested fibroblastic differentiation (Fig. 2B). In addition, the positive staining for vimentin (Fig. 2C) and the negative staining for cytokeratin (Fig. 2D) by immunohistochemical analysis revealed their mesenchymal origin. Taken together, these tumors generated by transformed BMMSCs were diagnosed as fibrosarcomas. BMMSCs have been shown to integrate into multiple organs after systemic administration as known as “homing” (11, 25). Therefore, we explored whether the transformed BMMSCs might similarly migrate to multiple organs when injected into immunocompromised mice through the tail vein. At 6-8 weeks post injection, transformed BMMSCs at P65 settled in several organs including lungs (Fig. 2E), kidneys (Fig. 2F), mediastinum (Fig. 2G), vertebrae (Fig. 2H), and pericardium (data not shown) with *in situ* tumorigenesis. Furthermore, we investigated whether fibrosarcoma cells isolated from tumors could regenerate tumors *in vivo*. Fibrosarcoma cells showed a clonogenic capability at the frequency of 2.4% from total dispersed fibrosarcoma cells (Fig. 2I). The progeny of twenty individual colonies was inoculated into secondary recipient immunocompromised mice

subcutaneously. All of these twenty colonies developed fibrosarcomas within 2 weeks (Fig. 2J). This evidence implies that a small population of fibrosarcoma cells, which forms colonies *in vitro*, maintains the properties of forming tumors upon serial transplantation as previously reported for cancer stem cells in other tumors (3-6).

Transformed BMMSCs at P57 sustained the expression of CD13 and Sca-1 (Fig. 2K), while they lost the expression of Thy-1, SSEA-1, and Flk-1 expressed in BMMSCs at P1 (data not shown). Hematopoietic cell markers, CD45, TER119, CD18, CD19, CD3, c-kit, and CD34, were negative in BMMSCs both at P57 and P1. These findings indicated that the transformation process changed the expression pattern of surface markers in BMMSCs but some markers expressed in BMMSCs at P1 were still maintained.

To further clarify the features of BMMSC at single cell level, single colony-derived BMMSCs were isolated and their immortalization and transformation potentials were assessed. We found that 5 out of 100 single colony-derived BMMSCs became immortalized. All of the immortalized clones maintained *in vitro* osteogenic differentiation potential and four out of five clones maintained *in vitro* adipogenic differentiation potential at early passages (Table 1). Four out of five of these clones were eventually transformed to generate fibrosarcoma following a subcutaneous inoculation (Table 1). One of them, clone C3, showed significant bone differentiation within the newly formed fibrosarcoma (Table 1). However, when transplanted with HA/TCP, two more clones (clone D2 and H8) also generated bone after they acquired tumor formation capacity (Table 1). These

findings suggest that not only multicolony-derived BMMSCs but also single colony-derived BMMSCs become transformed and that some cells in transformed clones partially maintain their differentiation capability, probably depending on the environment and the cell stages.

Accumulated chromosomal abnormalities were associated with the transformation of BMMSCs. It has been postulated that genome instability is critical for tumor formation (26, 27). We therefore examined chromosomal alterations in the transformed BMMSCs using the spectral karyotyping (SKY) analysis (18, 19) to find out the potential mechanism contributing to BMMSCs transformation. Fifty percent of BMMSCs showed normal chromosomes (40, XY) at P1, but displayed predominantly non-clonal numerical aberrations on remaining cells (Table 2), which may imply increased chromosome instability in murine BMMSCs. BMMSCs at P27 showed the gain of murine chromosome 2 (MMU2) in 40% of the cells (Fig. 3A and Table 2) and more than 10 double minute chromosomes per cell involving MMU15 in 40% of the cells (Fig. 3A, yellow arrow), indicating the existence of clonal numerical and structural abnormalities. Chromosomal aneuploidy was also detected with non-clonal gains and losses of numerous chromosomes (Table 2). At P55, BMMSCs showed a greater number of double minute chromosomes involving MMU15 in 90% of the analyzed cells (Fig. 3B, yellow arrow) and the clonal deletion of MMU14 (Fig. 3B and Table 2) with other numerical aberrations (Table 2). Chromosomal imbalances were more frequent at P55 compared to P27 (Table 2). These results suggested that accumulation of chromosomal abnormalities was a dynamic

process during continuous passages, leading to the immortalization and transformation of BMMSCs. We further performed fluorescence *in situ* hybridization (FISH) analysis and identified that the double minute chromosomes were due to an amplification of *c-myc*, an oncogene located on MMU15 (Fig. 3C). Western blot analysis confirmed the up-regulation of c-Myc protein expression in BMMSCs at P14, P29, and P54 when compared with the expression at P1 (Fig. 3D). Next, we examined telomerase activity since *c-myc* has been reported to activate telomerase activity (28, 29). The quantitative assay indicated that BMMSCs at P1 had little telomerase activity compared to the HEK293 cells used as a positive control, but following continuous passages, BMMSCs gradually gained increased telomerase activity (Fig. 3E). Non-transformed BMMSCs and transformed BMMSCs showed similar telomere lengths (Fig. 3F), suggesting that telomere length was maintained by telomerase activity during the immortalization and transformation process. These findings suggested that amplification of c-myc was, at least in part, involved in the transformation of BMMSCs through up-regulated telomerase activity.

Transformation system of BMMSCs can be utilized as a model for screening of anti-cancer drugs. Here we showed that transformed BMMSCs had quite different characteristics from their parental BMMSCs. We then selected two anti-cancer drugs, etoposide and doxorubicin, to compare how transformed BMMSCs and their parental BMMSCs might respond to treatment. After treatment with etoposide for 48 hours, the drug concentrations to suppress the cell viability to 50% of non-treated cells as a control (EC_{50}) are 185.54±21.20

μg/ml and 1.07±0.07 μg/ml (mean±SD) for BMMSCs at P1 and P63, respectively (Fig. 4A and 4B). The inhibitory curves of etoposide to BMMSCs at P1 and P63 were significantly separated (Fig. 4B), indicating that the therapeutic effect of etoposide may be achieved without causing a severe toxic effect on normal BMMSCs at a wide range of concentrations. In contrast, the inhibitory curves of doxorubicin to BMMSCs at P1 and P63 were very close. The mean EC_{50} of doxorubicin to BMMSCs at P1 and P63 were 0.49±0.18 μg/ml and 0.16±0.05 μg/ml, respectively (Fig. 4C and 4D), suggesting that the toxicity was relatively significant because there was no separation between “toxicity curve” (the inhibitory effect on BMMSCs at P1) and “effective curve” (the inhibitory effect on BMMSCs at P63). These findings may correlate with the fact that doxorubicin has adverse side effects on patients, such as the damage to cardiac muscles and the suppression of bone marrow function. Taken together, this system suggests a unique model for *in vitro* screening to select drugs and determine appropriate dosages to target transformed stem cells without severe side effects on normal stem cells.

Discussion

This study is the first report to show that murine BMMSCs can generate fibrosarcomas *in vivo* after spontaneous transformation into malignant cells. We clearly demonstrated the process from stem cells to malignant cells. Despite the assumption that the origin of cancer stem cells are related to postnatal stem cells, there has been no direct evidence to demonstrate that postnatal stem cells are involved in tumorigenesis. Here we provide direct evidence to show that murine BMMSCs could evolve into malignant tumors by spontaneous conversion of BMMSCs to transformed cells. The mechanism, by which BMMSCs are transformed into malignant cells, is correlated with accumulated chromosomal abnormalities, including structural and numerical aberrations, with increased passage numbers. Our data, including proliferation assay, histological analysis, chromosomal analysis, and quantitative telomerase activity assay, suggest that alteration of genome stability is a dynamic process, which may play a critical role to determine the fate of BMMSCs. More importantly, we showed the double minute chromosomes were present in the transformed BMMSCs, perhaps associated with elevated expression of c-Myc. Although many studies on human and murine cells have demonstrated a strong association between overexpression of c-Myc and tumorigenesis, this study is the first report to indicate that double minute chromosomes were developed during the transformation process of postnatal stem cells. In addition, we found that the tumors formed by transformed BMMSCs were pathologically identified as

fibrosarcomas. Transformed BMMSCs, which are a small population (5 of 100 single cell-derived clones) of adult BMMSCs, demonstrated unlimited population doublings, partially maintained differentiation capabilities *in vivo*, colonized in multiple organs after systemic injection, and obtained telomerase activity. These phenotypes are similar to MAPCs although transformed BMMSCs partially shared the expression profile of cell surface markers with MAPCs (11).

It is important to point out that the immortalization and transformation processes seen in murine BMMSCs were not observed in human BMMSCs under our culture conditions. To evaluate the potential of human BMMSCs to become spontaneously immortalized, we used similar strategies to find that *in vitro* cell culture with continuous passages led human BMMSCs to senescence without any sign of immortalization (data not shown). Human BMMSCs at P17, which had almost reached senescence, showed a very slow growth rate and demonstrated normal chromosomes (46, XX) in 14 of 15 analyzed cells, with only one revealing two non-clonal structural aberrations, deletion of chromosome 9 and 10 (data not shown). Therefore, human BMMSCs at the very latest stage of their life span are still capable of maintaining fidelity of chromosomal segregation. We tested not only human BMMSCs but also other human mesenchymal stem cells, including dental pulp stem cells (15) and periodontal ligament stem cells (16), and did not observe spontaneous immortalization (data not shown). Genome stability in human stem cells may be maintained with complicated mechanisms that keep human cells more stable than murine cells as previously reported (30). In the present study, murine BMMSCs at P1 showed high degree

of chromosome instability, implying that murine stem cells are susceptible to chromosomal aberration under *in vitro* cultivation which may associate with the clonal chromosomal abnormality such as increased gene amplification of c-myc. Very recently, however, the spontaneous transformation of human adult stem cell was reported (9). Although the mechanisms such as increased c-myc expression and telomerase activity may contribute to the spontaneous immortalization of human MSC (9) and murine BMMSCs, we have difficulty to immortalize human MSCs using the same continuous passage strategy as we did on murine BMMSCs. Even telomerase-transfected human BMMSCs can't be spontaneously immortalized under our experimental conditions (13). The discrepancy between the reported finding and our observation in human BMMSCs may be due to the different experimental conditions or the origin of donors. If human BMMSCs can be spontaneously transformed to malignant cells, the clinical applications of BMMSCs for tissue engineering should be conducted very carefully and new therapeutic approaches have to be developed to target transformed BMMSCs. Thus, understanding the mechanisms of how BMMSCs are transformed to malignant cells is very important for providing a new insight into therapeutic strategies when human stem cells are applied for clinical therapies.

Spontaneous immortalization/malignant transformation in our system may mimic the process of tumorigenesis in human body. Also, the comparison of BMMSCs with transformed BMMSCs derived from their parental normal BMMSCs makes this system unique to compare the response to the drugs at different stages. We attempted to utilize this BMMSCs/fibrosarcoma

transformation system to screen anti-cancer drugs for identifying a therapeutic index. The response of malignant cells and normal cells to drug treatment represents the effectiveness and the toxicity of the tested drug, respectively. After *in vitro* treatment, the EC_{50} of etoposide to normal BMMSCs at P1 was more than 170 folds higher than EC_{50} to transformed BMMSCs at P63, suggesting that etoposide has a wide therapeutic index. In contrast to etoposide, doxorubicin showed a very close EC_{50} between normal BMMSCs and transformed BMMSCs. These data suggest doxorubicin is more toxic than etoposide due to less specific effects on malignant cells. Indeed, this finding corresponds to the fact that doxorubicin causes worse side effects on patients, such as the damage to cardiac muscles and the suppression of bone marrow function. Taken together, it is suggested that this system has a potential to provide a useful model for *in vitro* drug screening. This may help us to examine newly developed drugs and select more appropriate drugs and dosages with avoiding severe side effects.

In summary, we demonstrated that murine BMMSCs become spontaneously transformed with accumulated chromosomal abnormalities including double minute chromosomes and form fibrosarcoma *in vivo*. Our BMMSCs/fibrosarcoma transformation system may be useful for drug screening as well as for further investigation of the mechanisms of how BMMSCs become transformed to establish the stem cell-based therapy.

Acknowledgement

We would like to thank Nicole McNeil (Genetics Branch, Center for Cancer Research, National Cancer Institute) for preparation of the *c-myc* probe for FISH analysis, Linda Barenboim Stapleton (Genetics Branch) for preparation of our mouse SKY probes, and Sivio Gutkind (Oral and Pharyngeal Cancer Branch/National Institute of Dental and Craniofacial Research) for critical reading and reviewing this manuscript. This work was supported by the intramural program of National Institute of Dental and Craniofacial Research, National Institutes of Health, Department of Health and Human Services.

References

1 Pardal R, Clarke MF, and Morrison SJ. Applying the principles of stem-cell biology to cancer. Nat Rev Cancer 2003;3:895-902.

2 Lapidot T, Sirard C, Vormoor J et al. A cell initiating human acute myeloid leukaemia after transplantation into SCID mice. Nature 1994;367:645-648.

3 Bonnet D, and Dick JE. Human acute myeloid leukemia is organized as a hierarchy that originates from a primitive hematopoietic cell. Nat Med 1997;3:730-737.

4 Hope KJ, Jin L, and Dick JE. Acute myeloid leukemia originates from a hierarchy of leukemic stem cell classes that differ in self-renewal capacity. Nat Immunol 2004;5:738-743.

5 Al-Hajj M, Wicha MS, Benito-Hernandez A et al. Prospective identification of tumorigenic breast cancer cells. Proc Natl Acad Sci U S A 2003;100:3983-3988.

6 Singh SK, Clarke ID, Terasaki M et al. Identification of a cancer stem cell in human brain tumors. Cancer Res 2003;63:5821-5828.

7 Singh SK, Hawkins C, Clarke ID et al. Identification of human brain tumour initiating cells. Nature 2004;432:396-401.

8 Houghton J, Stoicov C, Nomura S et al. Gastric cancer originating from bone marrow-derived cells. Science 2004;306:1568-1571.

9 Rubio D, Garcia-Castro J, Martin MC et al. Spontaneous human adult stem cell transformation. Cancer Res 2005;65:3035-3039.

10 Todaro GJ and Green H. Quantitative studies of the growth of mouse embryo cells in culture and their development into established lines. J Cell Biol 1963;17:299-313.

11 Jiang Y, Jahagirdar BN, Reinhardt RL et al. Pluripotency of mesenchymal stem cells derived from adult marrow. Nature 2002;418:41-49.

12 Miura M, Chen XD, Allen MR et al. A crucial role of caspase-3 in osteogenic differentiation of bone marrow stromal stem cells. J Clin Invest 2004;114:1704-1713.

13 Shi S, Gronthos S, Chen S et al. Bone formation by human postnatal bone marrow stromal stem cells is enhanced by telomerase expression. Nat Biotechnol 2002;20:587-591.

14 Lee HS, Huang GT, Chiang H et al. Multipotential mesenchymal stem cells from femoral bone marrow near the site of osteonecrosis. Stem Cells 2003;21:190-199.

15 Gronthos S, Mankani M, Brahim et al. Postnatal human dental pulp stem cells (DPSCs) in vitro and in vivo. Proc Natl Acad Sci U S A 2000;97:13625-13630.

16 Seo BM, Miura M, Gronthos S et al. Investigation of multipotent postnatal stem cells from human periodontal ligament. Lancet 2004;364:149-155.

17 Krebsbach PH, Kuznetsov SA, Satomura K et al. Bone formation in vivo: comparison of osteogenesis by transplanted mouse and human marrow stromal fibroblasts. Transplantation 1997;63:1059-1069.

18 Schrock E, du Manoir S, Veldman T et al. Multicolor spectral karyotyping of human chromosomes. Science 1996;273:494-497.

19 Liyanage M, Coleman A, du Manoir S et al. Multicolour spectral karyotyping of mouse chromosomes. Nat Genet 1996;14:312-315.

20 Fu B, Quintero J, and Baker CC. Keratinocyte growth conditions modulate telomerase expression, senescence, and immortalization by human papillomavirus type 16 E6 and E7 oncogenes. Cancer Res 2003;63:7815-7824.

21 Friedenstein AJ, Chailakhyan RK, Latsinik NV et al. Stromal cells responsible for transferring the microenvironment of the hemopoietic tissues. Cloning in vitro and retransplantation in vivo. Transplantation 1974;17:331-340.

22. Owen M and Friedenstein AJ. Stromal stem cells: marrow-derived osteogenic precursors. Ciba Found Symp 1988;136:42-60.

23 Prockop DJ. Marrow stromal cells as stem cells for nonhematopoietic tissues. Science 1997;276:71-74.

24 Pittenger MF, Mackay AM, Beck SC et al. Multilineage potential of adult human mesenchymal stem cells. Science 1999;284:143-147.

25 Liechty KW, MacKenzie TC, Shaaban AF et al. Human mesenchymal stem cells engraft and demonstrate site-specific differentiation after in utero transplantation in sheep. Nat Med 2000;6:1282-1286.

26 Feldser DM, Hackett JA, and Greider CW. Telomere dysfunction and the initiation of genome instability. Nat Rev Cancer 2003;3:623-627.

27 Mathon NF and Lloyd AC. Cell senescence and cancer. Nat Rev Cancer 2001;1:203-213.

28 Wang J, Xie LY, Allan S et al. Myc activates telomerase. Genes Dev 1998;12:1769-1774.

29 Wu KJ, Grandori C, Amacker M et al. Direct activation of TERT transcription by c-MYC. Nat Genet 1999;21:220-224.

30 Rangarajan A, Hong SJ, Gifford A, et al. Species- and cell type-specific requirements for cellular transformation. Cancer Cell 2004;6:171-183.

Figure Legends

Figure 1. Murine BMMSCs were transformed into malignant cells. (**A**) BMMSCs were cultured under standard condition and maintained over a year with over one hundred passages**.** They were considered as immortalized cells. (**B**) The proliferation rate was assessed by BrdU incorporation for 4 hours. The number of BrdU-positive cells was expressed as a percentage of the total number of counted cells at the indicated passages. BMMSCs at later passages showed a higher proliferating rate in comparison with BMMSCs at earlier passages with significant statistical difference ($*$; $p<0.05$, $n=10$). (**C**-**F**) BMMSCs at P1 maintain multiple differentiation capacity. Single colonies were formed after BMMSCs were plated at low density (1-2X10^6 cells/T-25 flask) and cultured with regular culture medium for ten days. Single colonies derived from BMMSCs were stained with 0.1% Tulidine blue (arrows, **C**). BMMSCs were cultured with 100 μM L-ascorbate-2-phosphate, 10 nM dexamethasone, and 2 mM β-glycerophosphate for 4 weeks. Alizarin red staining showed mineralized nodule formation (arrows, **D,** original magnification X100). Cultured BMMSCs formed Oil red O-positive lipid clusters following 3 weeks of induction in the presence of 0.5 μM isobutylmethylxanthine, 0.5 μM hydrocortisone, and 60 μM indomethacin (arrows, **E**, original magnification X400). When culture with TGF-β (2ng/ml), BMMSCs differentiated into chondrocytes with positive immunostaining of anti-type II collagen antibody (**F**, original magnification X400). (**G**-**N**) Immortalization and transformation of BMMSCs. BMMSCs at P1 (**G**) generated bones (*B*) and

associated hematopoietic elements (*BM*) upon transplantation into immunocompromised mice subcutaneously using HA/TCP (*HA*) (**K**). BMMSCs at P13 showed enlarged shape (**H**) and failed to generate any mineralized tissue upon *in vivo* transplantation. Only fibrous tissue (*F*) was presented around HA/TCP (*HA*) (**L**). BMMSCs at P29 became smaller (**I**) and showed tumor formation when transplanted into immunocompromised mice (*T*, **M**). BMMSCs at P54 showed significant smaller shape (**J**) and generated tumors with higher cell density and shorter latent periods compared with BMMSC at P29 when transplanted into immunocompromised mice (*T*, **N**). (**G**-**J**) 0.1% Toluidine blue staining. Original magnification X200. (**K**-**N**) H&E staining. Original magnification X200.

Figure 2. Transformed BMMSCs generated fibrosarcomas and colonized in multiple organs. (**A**-**D**) Histology of tumors generated by BMMSCs at P67. Tumors were composed of spindle and round atypical cells and invasive to surrounding muscles (arrow). Mitosis of nuclei was also observed (yellow arrow) (**A**). Mallory trichrome staining showed fibroblastic differentiation of tumor cells (blue staining). Red color staining (arrows) indicated the muscles (**B**). Immunohistochemical staining using anti-vimentin antibody indicated that the tumor cells originated from mesenchymal cells (arrow heads) (**C**). Negative staining using anti-cytokeratin antibody (star) excluded possibility of epithelial cell origin of the tumor cells. Skin epidermal tissues were positive for cytokeratin (arrows) (**D**). (**A**-**D**) Original magnification X200. (**E**-**H**) Transformed BMMSCs at

P65 showed tumor formation (*T*) in alveolar spaces of lungs (*L*, **E**), kidney (**F**), mediastinum (**G**) and vertebrae (**H**) following intravenous injection into mice. Gromelurus (*G*), renal tubules (*Tu*), trachea (*Tr*), tracheal cartilages (*TC*), bone (B). (**E**-**H**) H&E staining. Original magnification X200. **(I)** Single cells from dispersed fibrosarcomas formed colonies *in vitro* and (**J**) re-formed tumors in the second recipients when $1x10^6$ cells were inoculated. (**K**) FACS analysis indicated that transformed BMMSCs were positive for CD13 and Sca-1, but negative for Thy-1, SSEA-1, Flk-1, and hematopoietic markers; CD45, TER119, CD18, CD19, CD3, c-kit, and CD34.

Figure 3. Chromosomal abnormalities in transformed BMMSCs. (**A**) SKY analysis of BMMSCs at P27 showed a gain of chromosome MMU2 and double minute chromosomes involving MMU15 (yellow arrow). (**B**) SKY analysis of BMMSCs at P55 indicated a significant increase in the number of double minutes involving MMU15 (yellow arrow). Deletion in MMU14 and a loss of MMU8 were noted. (**C**) FISH analysis revealed an amplification of *c-myc* (yellow arrows) located on MMU15 (white arrows). (**D**) Western blot analysis confirmed the up-regulated expression of c-Myc in BMMSCs at P14, P29, and P54 when compared to BMMSCs at P1. (**E**) BMMSCs gradually gained significant telomerase activity following continuous passages ($*$; $p<0.05$, n=3). HEK293 cells were used as a positive control (c). (**F**) Telomere length of BMMSCs was not significantly changed during the continuous passages from P1 to P90.

Figure 4. Normal and transformed BMMSCs responded differently to anti-cancer drugs. Cell viability of BMMSCs at P1 and P63 was evaluated after anti-cancer drug treatment. (**A**, **B**) Treatment with etoposide (0-1000 μg/ml) for 48 hours. BMMSCs at P1 and P63 seeded in 96-well plates were treated with the indicated concentration of etoposide. The representative plate demonstrated gradual changing of color with increased concentrations of etoposide. The change of color was more drastic in P63 compared to P1 (**A**). The inhibitory curves to BMMSCs at P1 (black solid line) and P63 (blue dotted line) were significantly separated, indicative of a wide therapeutic index (**B**). (**C**, **D**) Treatment with doxorubicin (0-30 μg/ml) for 48 hours. The color of plate was changed similarly at P1 and P63 (**C**). There was no separation between “toxicity curve” (the inhibitory effect on BMMSCs at P1) and “effective curve” (the inhibitory effect on BMMSCs at P63) (**D**).

Clone	Osteo. (~P13)	Adipo. (~P13)	Tumor formation (passage stage)	Histological finding of tumor by subcutaneous injection	Bone formation in transplants with carrier
A8	+	±	-	-	-
B10	+	+	+ (~P88)	fibrosarcoma	-
C3	+	-	+ (~P66)	fibrosarcoma / bone formation	+
D2	+	±	+ (~P65)	fibrosarcoma	+
H8	+	+	+ (~P29)	fibrosarcoma	+

Table 1; Characteristics of single colony-derived BMMSC clones

Only 5 clones (A8, B10, C3, D2, and H8) from 100 single colony-derived BMMSC clones were spontaneously immortalized. Osteogenic and adipogenic differentiation capacities were examined by alizarin red staining and oil red O staining, respectively at early passages. All immortalized BMMSC clones except A8 clone formed tumors at different passages when inoculated into immunocompromised mice subcutaneously. One clone (C3) showed bone formation along with fibrosarcoma components upon inoculation and another two clones (D2 and H8) generated bone after malignant transformation only when transplanted with HA/TCP as a carrier.

		Chromosome																			
		1	2	3	4	5	6	7	8	9	10	11	12	13	14	15	16	17	18	19	X	Y
P1	Loss of 1 copy				1				1	1									1			
	Gain of 1 copy																1				1	
	Deletion			2																		
P27	Loss of 1 copy	1					1			1	1		1	1	1		1	1	1			
	Gain of 1 copy		4			1	1		1					1								
P55	Loss of 1 copy		2	1			1		1			1	1									2
	Loss of 2 copies															1		1				
	Gain of 1 copy	1				1					1	1							2		1	2
	Deletion						1			1					5							
	Acentric fragment		1				1															
	Dicentri	1																				

Table 2; The numerical chromosomal aberrations observed in 10 BMMSCs at P1, P27, and P55

Ten chromosomal specimens from BMMSCs at P1, P27, and P55 were analyzed by SKY and the number of specimens showing the numerical aberrations was summarized. BMMSCs at P27 exhibited clonal gains (>2) of MMU2. BMMSCs at P55 demonstrated clonal deletions (>3) of MMU14. Chromosomal aneuploidy with non-clonal gains and losses of numerous chromosomes was accumulated in BMMSCs at P55 compared with earlier stage cells. Our cytogenetic interpretations follow the guidelines specified in The Jackson Laboratory ; Mouse Genome Informatics, Mouse Nomenclature Guidelines & Locus Symbol Registry (www.informatics.jax.org/mgihome//nomen/index.shtml).

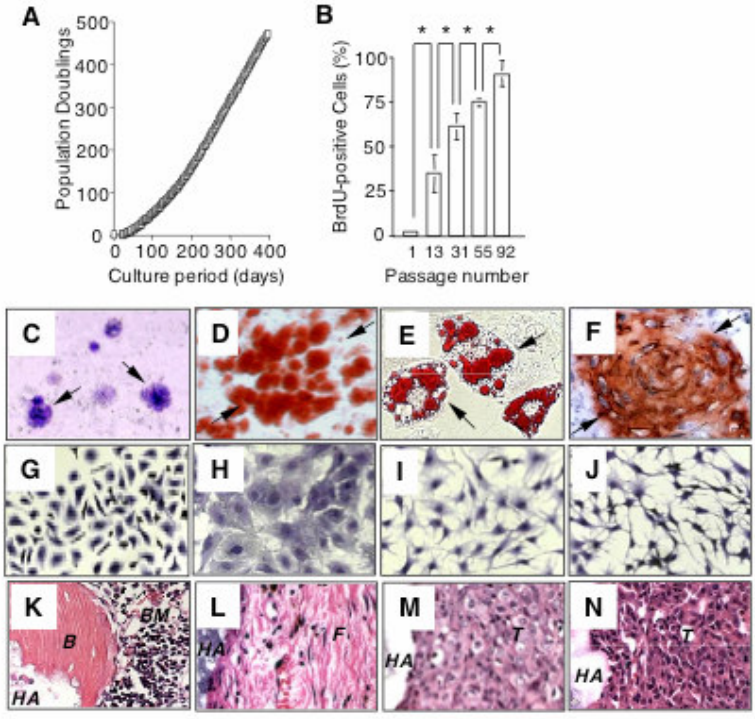

Figure 1

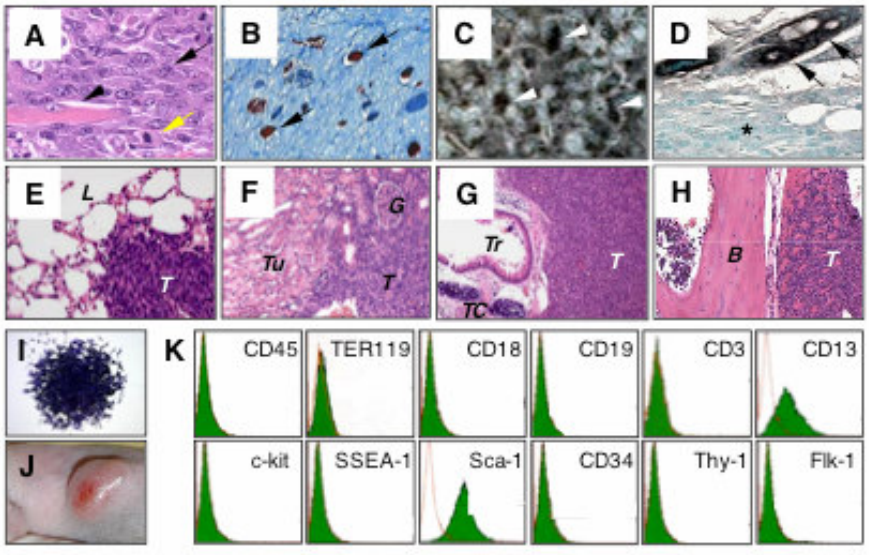

Figure 2

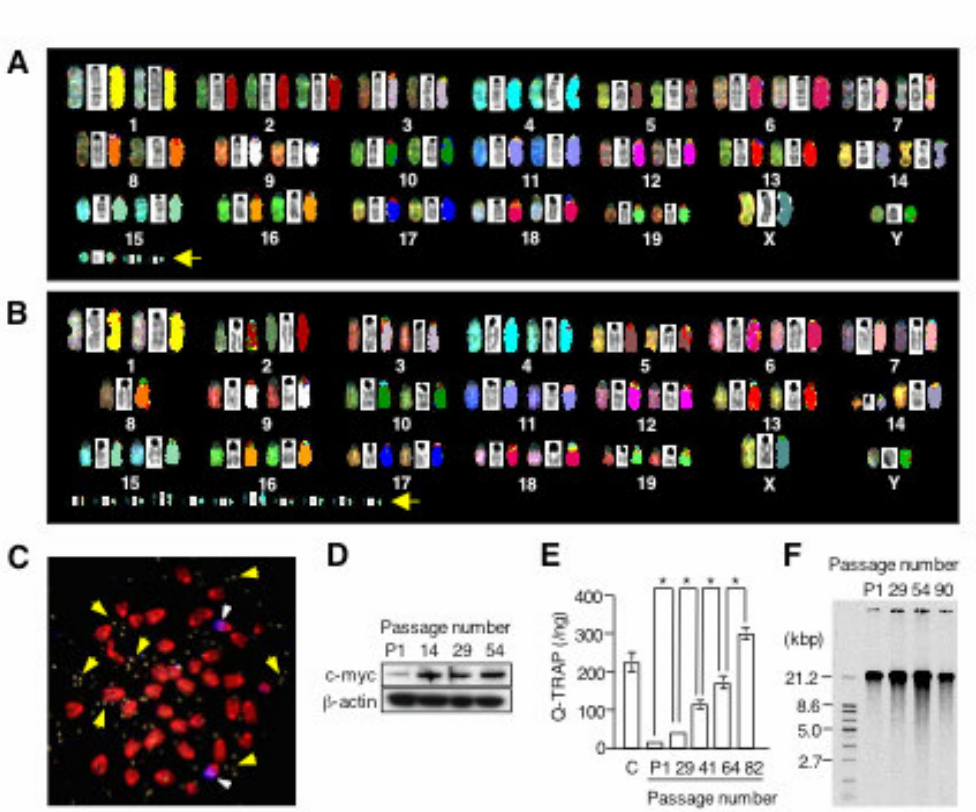

Figure 3

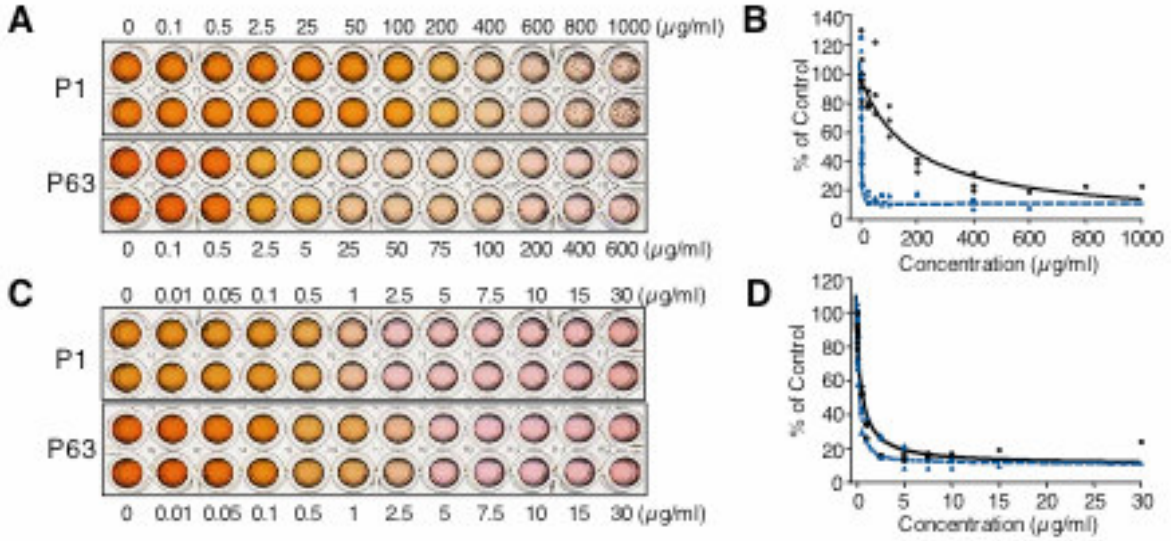

Figure 4